https://doi.org/10.5194/hess-2021-470
Preprint. Discussion started: 29 September 2021

Hydrology and Earth System Sciences
Discussions

A Time-Varying Distributed Unit Hydrograph considering soil moisture content

Bin Yi[1,2], Lu Chen[1,2*], Hansong Zhang[3], Ping Jiang[4], Yizhuo Liu[1,2], Hongya Qiu[1,2]

[1] *School of Civil and Hydraulic Engineering, Huazhong University of Science and Technology, Wuhan, 430074, China*

[2] *Hubei Key Laboratory of Digital Valley Science and Technology, Wuhan 430074, China*

[3] *PowerChina Huadong Engineering Corporation Limited，Hangzhou 310014, China*

[4] *Meizhou Hydrological Bureau, Guangdong Province, Meizhou 514000, China*

Correspondence: Lu Chen (chen_lu@hust.edu.cn)

Abstract: The distributed unit hydrograph (DUH) method has been widely used for flood routing simulation, because it can well characterize the underlying surface characteristics and various rainfall intensities. The core of the DUH is the calculation of flow velocity. However, the current velocity formula assumed a global equilibrium of the watershed and ignored the impact of time-varying soil moisture content on flow velocity, which leads to a larger flow velocity value. The goal of this study is to identify a soil moisture content factor, which was derived based on the water storage capacity curve, to explore the responses of DUH to soil moisture content in unsaturated areas. Thus, an improved distributed unit hydrograph based on time-varying soil moisture content was proposed in this paper. The proposed method considered the impact of both the time-varying rainfall intensity and soil moisture content on the flow velocity, and the watershed is assumed not to be equilibrium but vary with the soil moisture. The Qin River Basin was selected as a case study, and results of the time-varying distributed unit hydrograph (TDUH) and current DUH methods were used as comparisons with that of proposed method. Influence mechanism of time-varying soil moisture content on the flow velocity and flood forecasts were explored. Results show that the proposed method performs the best among the three methods. The shape and duration of the unit hydrograph can be mainly related to the soil moisture content at initial stage of a storm. When the watershed is approximately saturated, the grid flow velocity is majorly dominated by the excess rainfall.

Keywords: Time-varying distributed unit hydrograph, Runoff routing, Flow velocity, Soil moisture content, Excess rainfall

1. Introduction

Flood is a natural disaster with strong suddenness, high frequency and serious harm (Jongman et al., 2014; Alfieri et al., 2015; Munich, 2017). Global flood losses account for about 40% of the total losses of all kinds of natural disasters. High accuracy flood forecasts can provide decision-making basis for reservoir operation, flood control, and optimal allocation of water resources, which plays a significant role in water resources management, development and utilization, and national economic construction.

Watershed routing calculation is an important procedure in hydrological model, whose accuracy directly affects flood forecasts results. The Unit Hydrograph (UH), proposed by Sherman (1932), is one of the methods most widely used for development of flood prediction and warning systems for gauged basins with observed rainfall–runoff data (Singh et al., 2014). The UH is a surface runoff hydrograph resulting from one unit of rainfall excess uniformly distributed spatially and temporally over the watershed for the entire specified rainfall excess duration (Chow 1964). Usually, the UH can be categorized into 4 major types, including the traditional models, probability models, conceptual models, and geomorphologic methods (Bhuyan et.al. 2015).

First, the traditional models were discussed. The traditional methods established the relationships between parameters used to describe the UH (e.g. peak flow, time to peak and time base) and parameters used to describe the basin. Snyder (1938), Mockus (1957), and U.S. Soil Conservation Service (SCS) (2002) proposed some traditional methods,, which are still available to hydrologists nowadays. The disadvantages of these methods are that they do not yield satisfactory results, and their application to practical engineering problems is tedious and cumbersome (Nigussie et al., 2016).

Furthermore, Most UHs have steeper rising limbs than their receding sides, which can be well characterized by the probability distribution functions (pdfs). Many pdfs were used for derivation of UHs due to their similarity in the shape of statistical distributions to UHs. The difficulties of these methods are that the distribution functions are diverse, and the parameters depends on numerous hydrological data (Bhuyan et al., 2015).

https://doi.org/10.5194/hess-2021-470
Preprint. Discussion started: 29 September 2021

Hydrology and Earth System Sciences
Open Access
Discussions

Another modeling technique for deriving UHs is conceptual model. Nash (1957) proposed a conceptual model characterized as a succession of *n* linear reservoirs connected in series with the same storage coefficient *K*, for the derivation of the instantaneous unit hydrograph (IUH). After that, Dooge (1959) derived a mathematical model for the IUH based on linear reservoirs. Bhunya et al. (2005) and Singh et al. (2007) represented a hybrid and extended hybrid model based on the linear reservoir model. Singh (2015) proposed a new simple two-parameter IUH with conceptual and physical justification. Khaleghi et al. (2018) suggested a new conceptual model namely the inter-connected linear reservoir model (ICLRM). However, the conceptual model neglects the impact of uneven spatial distribution of the basin's underlying surface on the UHs.

On the bases of time-area method developed by Clark (1945), Rodriguez-Iturbe (1979) proposed a geomorphologic instantaneous unit hydrograph (GIUH) method, which couples the hydrologic characteristics of a catchment with more detailed geomorphologic parameters (Kumar et al., 2007). In the model, the IUH corresponds to the probability density function of travel times from the locations of runoff production to the outlet of a watershed (Gupta et al., 1980). With the development of digital elevation models (DEMs) and geographic information system (GIS) technology, the formulation of width function-based geomorphological IUH methods are available, the rigidity of which is reflected in its incapacity to account properly (i.e. to respect the geometry) for the distribution of rainfall (Rigon et al., 2016).

https://doi.org/10.5194/hess-2021-470
Preprint. Discussion started: 29 September 2021

The methods mentioned above are based on the UH linear assumption. However, it is well-known that the rainfall-runoff process is nonlinear due to the dependence of the flood wave celerity on the excess rainfall intensity (Robinson et al., 1995). Minshall (1960) showed that different rainfall intensities significantly correspond to different UHs for a small watershed. After that, Rodríguez-Iturbe et al. (1982) extended the GIUH to the geomorphoclimatic IUH (GcIUH) to cope with this nonlinearity by incorporating excess rainfall intensity in the determination of the IUH. Lee et al. (2008) proposed a variable Kinematic wave GIUH corresponding to time-varying rainfall intensity for the calculation of the runoff concentration, which warrants consideration for rainfall-runoff modelling in ungauged catchments that are influenced by high intensity rainfall.

Furthermore, it is difficult for the previous methods (traditional models, probability models, conceptual models, and geomorphologic models) to fully consider the geomorphic characteristics of the watershed while incorporating the nonlinearity of rainfall-runoff process (e.g. time-varying rainfall intensities). Thus, the spatially distributed unit line hydrograph (DUH) method has been attached much attention. The concept of a DUH is based on the fact that the unit hydrograph can be derived from the time-area curve of a watershed by the S-curve method (Muzik, 1996). The DUH can be essentially classified as a type of geomorphoclimatic unit hydrograph, since its derivation depends on watershed geomorphology, rainfall and hydraulics (Du et al., 2009). The spatially distributed flow celerity and temporally varying excess rainfall intensities can be considered in this method (Bunster et al., 2019).

In DUH models, the travel time of each grid cell can be calculated by dividing the travel distance of a cell to the next cell by velocity of flow generated in that cell (Paul et al., 2018). And the travel times are then summed along the flow path to obtain the total travel time from each cell to the outlet. The DUH can be derived using the distribution of travel time from all grid cells in a watershed (Bunster et al., 2019). Some DUH models assumed a time-invariant travel time field and ignored the dependence of travel time on excess rainfall intensity (Melesse & Graham, 2004; Noto and La Loggia, 2007; Gibbs et al., 2010), while others suggested various UHs correspond to different storm events, namely time-varying distributed unit hydrograph (TDUH) (Martinez et al.,2002; Sarangi et al., 2007; Du et al., 2009). Compared to the fully distributed models based on the momentum equation, DUH model is a more efficient approach that allow the use of distributed terrain information in a purely ungauged region. The DUH methods are better than the traditional UHs because the spatially information of watershed and time-varying rainfall-runoff process was considered, and have been developed as an alternative method to semi-distributed and fully distributed methods for rainfall-runoff modelling (Bunster et al., 2019).

Many researchers have also focused on the upstream contributions to the travel time estimation besides excess rainfall intensity in TDUH method. For instance, Maidment et al. (1996) defined the velocity in the cell also as a function of the contributing area to take into accounts the velocity increase observed downstream in

https://doi.org/10.5194/hess-2021-470
Preprint. Discussion started: 29 September 2021

river systems (Gironás et al., 2009). Gad (2014) applies a grid-based technique implementing the stream power formulation to relate flow velocity to the hydrologic parameters of the upstream watershed area through simplistic parametric approaches. Many similar works have been done by Saghafian and Julien (1995), Bhattacharya et al. (2012) and Chinh et al. (2013). Yet, they assumed that the watershed was global equilibrium. After that, Bunster et al. (2019) developed a spatially TDUH model that accounts for dynamic upstream contributions and characterized the temporal behavior of upstream contributions and its impact on travel times in the basin. However, this time-varying DUH model also adopted the assumption that equilibrium in each individual grid cell can be reached before the end of the rainfall excess pulse. When there accrues continuous excess-rainfall in a watershed, the soil moisture content and surface runoff increase, and the infiltration rate decreases, leading to an acceleration of the routing velocity. Until the entire basin is saturated and the routing velocity reach its maximum. Accepting the assumption of equilibrium in global or the grid cell yields slower travel times, shorter times to peak, and higher peak discharges. However, all the aforementioned approximations neglect the impact of dynamic changes of soil moisture exchange and water storage in unsaturated regions.

The objective of this study is therefore to propose a time varying distributed unit hydrograph runoff routing method that accounts for dynamic rainfall intensity and soil moisture content based on the existing Xinanjiang (XAJ) model. The main contributions and innovations of the present study are as follows. First, the soil moisture

https://doi.org/10.5194/hess-2021-470
Preprint. Discussion started: 29 September 2021

content proportional factor in the unsaturated area was identified and expressed based on the water storage capacity curves. Second, the travel time expression function based on the Kinematic wave theory was modified by considering a soil moisture content proportional factor. Besides the rain intensity, the influence of the time-varying soil moisture storage on the confluence velocity was considered in the watersheds, where the runoff generation is dominated by saturation-excess mode. Finally, the Qin River Basin in Guangdong Province, China, was selected as a case study. The TDUH and DUH methods were compared with the proposed method.

https://doi.org/10.5194/hess-2021-470
Preprint. Discussion started: 29 September 2021

2. Establishment of flood forecasts model

The flood forecast modelling frame work mainly consists the calculation of excess rainfall and the derivation of DUH. In this study, the XAJ model was adopted to calculate the excess rainfall and a new routing method was developed to incorporate the behavior of dynamic changes of soil moisture content and rainfall intensity. The soil moisture content factor in unsaturated regions was expressed by the water storage capacity curves. Thus, the individual gird cell was not assumed to be equilibrium but variable in time. The general formula of velocity proposed by Madidement (1993) combining with the soil moisture content factor was proposed for considering the impact of underlying spatially heterogeneous on the watershed equilibrium.

2.1 Calculation of runoff generation

The Xinanjiang (XAJ) model was used for the calculation of excess rainfall in this study. It is a conceptual hydrologic model proposed by Zhao et al. (1980) for flood forecasts in the Xinan River Basin. After that, the XAJ model has been widely used in humid and semi-humid watersheds all over the world (Zhao, 1992). It mainly consists of four modules, namely evapotranspiration module, runoff generation module, runoff partition module and runoff routing module (Zhou et al., 2019). Usually, a large watershed is divided into several sub-watersheds to capture the spatial variability of underlying surface, precipitation, and evaporation. In each sub-basin, the inputs of the XAJ model are the average areal rainfall as well as evaporation, and the output is streamflow. The schematic diagram of the XAJ model is shown in Figure 1.

First, for the evapotranspiration module, the soil profile of each sub-basin is divided into three layers, the upper, lower and deeper layers, and only when the layer above it exhausted water does evaporation from a next layer occur. Second, as for the Runoff generation in the XAJ model, a catchment is divided into two parts by the percentage of impervious and saturated areas, namely permeable and impervious areas respectively. Since the soil moisture deficit is heterogeneous, runoff distribution is usually nonuniform across a basin. Thus, a storage capacity curve was adopted by the XAJ model to accommodate the nonuniformity of the soil moisture deficit or the tension water capacity distribution. Third, the runoff partition of the XAJ model divides the total runoff into three components by a free reservoir, which consists of surface runoff (RS), interflow runoff (RI) and groundwater runoff (RG). More details can be found in (Zhao et al., 1980). Finally, the linear reservoir method was adopted for calculation of catchment routing (Lu et al., 2014), and the TDUH considering soil moisture content, DUH, TDUH were used to calculate the routing of river net. The Maskingen method was employed to produce the streamflow from each sub-basin to the outlet of the entire catchment. Various runoff routing methods were introduced in Section 2.2.

2.2 Calculation of runoff routing based on TDUH considering time-varying soil moisture content

The routing calculation adopted the GIS-derived DUH method, which allowed the velocity to be calculated on a grid cell basis over the catchment. The core of the DUH

https://doi.org/10.5194/hess-2021-470
Preprint. Discussion started: 29 September 2021

Hydrology and Earth System Sciences
Open Access
Discussions

method is to equate the probability density distribution function of the time at which the rainfall flows to the outlet of the basin to the IUH, in which the time-area relationship was derived using the velocity field with spatial distribution characteristics. Laurenson (1964) identified that the concept of DUH was due to time-area histogram. After that, Madidement (1993) proposed the travel time formula for each grid cell, which are relating to the length, slop, velocity coefficient of any reach of the flow path, expressed as Equations. (1) and (2). The diagram of travel time calculation is shown as Figure 2(a).

$$V = kS^{0.5} \tag{1}$$

$$\Delta\tau_i = \frac{L_i}{V_i} \quad \text{or} \quad \Delta\tau_i = \frac{\sqrt{2}L_i}{V_i} \tag{2}$$

where V is the flow velocity; S is the slope of the watershed unit; k is the coefficient of the flow velocity which is related to the vegetational form of the watershed unit; $\Delta\tau_i$ is the retention time of the unit i; L_i is the path length of the stream; and m is the number of the watershed unit.

Then the simulation is performed along the flow path from the gird cell to the watershed outlet (Muzik, 1996), and the formula is given by

$$\tau = \sum_{i=1}^{m} \Delta\tau_i \tag{3}$$

where τ_i is the travel time from the unit i to the outlet of the sub-watershed.

In addition, the time-area histogram of the watershed can be obtained after the arrival time of each cell being calculated as shown in Figure2 (b), which indicates the

https://doi.org/10.5194/hess-2021-470
Preprint. Discussion started: 29 September 2021

distribution of partial watershed areas contributing to runoff at the watershed outlet as a function of travel time (Muzik, 1996). The time-area diagram can be obtained based on the distribution of travel time, namely S-hydrograph, as shown in Figure 2(c). Then, the DUH can be derived from the S-hydrograph. The time-area diagram values are at discrete time points, and the specific formula is given by

$$UH\left(i\Delta t\right)=\frac{A\left(i\Delta t\right)-A\left[\left(i-1\right)\Delta t\right]}{\Delta t} \tag{4}$$

where ($t=i\Delta t$ and i = 0, 1, 2, ..., n); UH is the ordinate value of the DUH; $A\left(i\Delta t\right)$ is the total area of the watershed; Δt is the time interval.

However, the methods above only consider the influence of the spatial heterogeneity of the underlying surface on the catchment routing process and adopt a single UH for each sub-watershed, ignoring the effect of time-varying rain intensity. Thus, the TDUH can be derived by combining the continuity and Manning equations (Noto & Loggia, 2007). Compared to the traditional DUH method, the TDUH method is more consistent with the routing process. The concrete derivation process of this method is as follows.

The continuity equation of water flow is given by

$$VLh=IA \tag{5}$$

where V is the velocity of the flow; L is the length of the unit; h is the depth of the stream; I is the intensity of the excess rainfall; and A is the area of the unit, $A=L^2$.

The Manning formula is described by

https://doi.org/10.5194/hess-2021-470
Preprint. Discussion started: 29 September 2021

$$V = \frac{1}{n} h^{\frac{2}{3}} S^{\frac{1}{2}} \tag{6}$$

where n is the coefficient of the roughness; and S is the slope of the watershed unit.

Combining Equations. (5) and (6), the specific formula of the flow velocity can be written by

$$V = \frac{1}{n^{0.6}} I^{0.4} L^{0.4} S^{0.3} \tag{7}$$

Denote the discrete rainfall intensity and the reference rainfall intensity as I_s and I_c respectively (Kong et al., 2019). The flow velocity of the discrete rainfall intensity V_s can be written by

$$V_s = V_c \cdot \frac{V_s}{V_c} = V_c \cdot \frac{I_s^{2/5}}{I_c^{2/5}} \tag{8}$$

where V_c is the flow velocity of the reference rainfall intensity.

Combining Equations. (6) and (8), the flow velocity formula considering rainfall intensity is given by

$$V_{s1} = \frac{1}{n} h^{\frac{2}{3}} S^{\frac{1}{2}} \left(\frac{I_s}{I_c}\right)^{\frac{2}{5}} v = kS^{\frac{1}{2}} \left(\frac{I_s}{I_c}\right)^{\frac{2}{5}} \tag{9}$$

where k is the velocity coefficient.

Equation. (5) assumes that equilibrium in each individual grid cell is reached before the excess rainfall pulse. However, the DUH derived based on this assumption may be higher, leading to larger forecast errors. For instance, in a continues storm event, due to the spatial heterogeneity of the underlying surface, the surface runoff increases in the unsaturated regions, and the infiltration rate decreases. As is known that the more

https://doi.org/10.5194/hess-2021-470
Preprint. Discussion started: 29 September 2021

surface runoff, the greater the velocity. Until the entire basin is saturated and the routing velocity reach its maximum. However, the traditional velocity calculations do not consider the influence of the proportion of water sources in the unsaturated area on the flow velocity. To solve this issue, an improved TDUH method considering soil moisture content was proposed in this paper. The proposed equations for calculation of the flow velocity of each cell was discussed below.

First, combining the soil moisture content and watershed storage capacity curve to calculate α_t (the fraction of basin with the soil storage capacity less than W_t); Furthermore, for the $(1-\alpha_t)$ part, calculating the proportion of A_t (the current soil moisture content) to $A_t + B_t$ (the corresponding maximum soil moisture storage for part of $(1-\alpha_t)$). The schematic diagram is shown in Figure 3, in which $\alpha \sim WM^{'}$ is the watershed storage capacity curve; W_t is the current soil moisture storage; and $(1-\alpha_t)$ is the part of the watershed that the soil moisture storage dose not reach the maximum.

For the watershed storage capacity curve $\alpha \sim WM^{'}$, the specific formula is given by

$$\alpha = 1 - \left(1 - \frac{WM^{'}}{WMM}\right)^{b} \tag{10}$$

where $WM^{'}$ is the soil storage capacity of the watershed; WMM is maximum watershed soil storage capacity; α is fraction of basin with the soil storage capacity less than $WM^{'}$; and b is exponent of the curve.

https://doi.org/10.5194/hess-2021-470
Preprint. Discussion started: 29 September 2021

Hydrology and Earth System Sciences
Discussions

For the current soil moisture storage content of the $(1-\alpha_t)$ part, the specific formula is given by

$$A_t = 1-\alpha_t \cdot W_t \tag{11}$$

For the maximum soil moisture storage of the $(1-\alpha_t)$ part, the specific formula is given by

$$A_t + B_t = \int_{\alpha_t}^{1} WMM\left[1- \ 1-\alpha^{\frac{1}{b}}\right]d\alpha \tag{12}$$

Thus, the proportion w_t of the current soil moisture content to the corresponding maximum soil moisture content is expressed by

$$w_t = \frac{A_t}{A_t + B_t} = \frac{1-\alpha_t \cdot W_t}{\int_{\alpha_t}^{1} WMM\left[1- \ 1-\alpha^{\frac{1}{b}}\right]d\alpha} = \frac{W_t}{WMM\left[1-\frac{b}{b+1} \ 1-\alpha_t^{\frac{1}{b}}\right]} \tag{13}$$

It can be seen from Equation. (13) that as the rainfall continuous, the soil moisture content in the unsaturated area continues to increase and the non-runoff area continues to decrease. With the gradual increase of soil moisture content w_t, (1-α_t) approaches 0 and w_t tends to 1 when the basin reaches the full storage.

Combining Equations. (9) and (13), and considering the impact of both rainfall intensity and time-varying soil moisture content on the watershed velocity, the velocity equation is assumed to be

$$V_{s2} = k \cdot S^{\frac{1}{2}} \cdot \left(\frac{I_s}{I_c}\right)^{\frac{2}{5}} \cdot w_t \tag{14}$$

Similar to the studies on dynamic upstream contributions by Bhattacharya et al. (2012), Bunster et al. (2019), a power law can be used to improve the applicability of

https://doi.org/10.5194/hess-2021-470
Preprint. Discussion started: 29 September 2021

it, and the formula is expressed by

$$V_{s2} = k \cdot S^{\frac{1}{2}} \cdot \left(\frac{I_s}{I_c}\right)^{\frac{2}{5}} \cdot w_t^{\gamma} \tag{15}$$

where γ is an exponent smaller than unity, which needs to be determined by trial and error method. Hence, the fraction of the current soil moisture content w_t that contributes to the flow velocity decreases as w_t increases.

Therefore, the proposed method considering both the rainfall intensity and soil moisture content was proposed, in which soil moisture content is regarded as an important factor affecting the TDUH. When the soil moisture content of the whole basin reaches the saturation, V_{s2} is equal to V_{s1}.

2.3 Model calibration

The SCE-UA (Shuffled Complex Evolution Algorithm) method, developed by the University of Arizona in1992 (Duan et al., 1992), is suitable for the nonlinear, high dimension optimization problems. The method has been widely used for the calibration of hydrological model (Vrugt et al., 2006; Beskow et al., 2011; Zhou et al., 2018). Hence, the SCE-UA method was used to optimize the parameters of XAJ model in this study. The relative flood peak error, relative peak time error, and Nash-Sutcliffe efficiency of floods were chosen as the criteria, the specific functions of which are given as follows.

(a) Objective function of the flood peak:

https://doi.org/10.5194/hess-2021-470
Preprint. Discussion started: 29 September 2021

$$Obj_1 = \frac{1}{N}\left|\sum_{i=1}^{N}\left(\frac{Q'_{obs,i} - Q'_{sim,i}}{Q'_{obs,i}}\right)\right| \tag{16}$$

(b) Objective function of the peak time error:

$$Obj_2 = \left|\sum_{i=1}^{n}\left(T_{obs,i} - T_{sim,,i}\right)\right| / \left(\sum_{i=1}^{n} T_{obs,i}\right) \tag{17}$$

(c) Objective function of the Nash-Sutcliffe efficiency:

$$NSE = 1 - \left[\sum_{i=1}^{n}\left(Q_{obs,i} - Q_{sim,i}\right)^2\right] / \left[\sum_{i=1}^{n}\left(Q_{obs,i} - \overline{Q}_{obs}\right)^2\right] \tag{18}$$

$$Obj_3 = 1 - NSE \tag{19}$$

(d) The optimized objective function:

$$Obj = \min(aObj_1 + bObj_2 + cObj_3) \tag{20}$$

where $Q_{obs,i}$ is the value of actual flood flow; $Q_{sim,i}$ is the value of predicted flood flow; $Q'_{obs,i}$ is the value of actual flood peak; $Q'_{sim,i}$ is the value of predicted flood peak; $T_{obs,i}$ is the time of actual flood peak; $T_{sim,,i}$ is the time of predicted flood peak; $\overline{Q}_{obs}$ is the average of actual flood flow; N is the number of the flood; a, b and c are constants.

3 Study area and data

The Qin River basin was selected as a case study. This river is the tributary of the Mei jiang River, which originates from Guangdong Province, China. The Qin River is 91 km long with a basin area of 1578 km^2. The mean slope of the basin is 1.1‰. There are 21 meteorological stations and 1 flow station (Jianshan station) in this area. The location and stations of the Qin River Basin are shown in Figure 4.

https://doi.org/10.5194/hess-2021-470
Preprint. Discussion started: 29 September 2021

According to the DEM data of the Qin River Basin, the whole basin can be divided into 9 sub-watersheds based on the natural water system, namely watershed 1-9 from upstream to downstream as shown in Figure 5. The details of each sub-watershed are given in Table 1.

The rainfall and evaporation data from meteorological stations was collected with the length from the years 2013 to 2018. The simultaneous hourly runoff data for the Jianshan station was collected as well. The soil moisture content before the floods was calculated based on the daily recession coefficient of water storage in the basin.

4. Results and discussions

4.1 Calibration of parameters

4.1.1 Parameters Calibration of the runoff generation using the XAJ Model

The accuracy of runoff generation calculation is of great importance in the rainfall-runoff forecasts. The higher the accuracy of the runoff calculation is, the smaller the impact on the error of the routing calculation is. Because the Qin River Basin is in the humid area of southern China, the saturation-excess method with three-source runoff separation of the XAJ model was adopted to calculate the excess rainfall in this study. Dozens of floods were selected to calibrate the parameters of the XAJ model by the shuffled complex evolution algorithm method. In addition, to make the simulation results of the XAJ model more accurate, the unit hydrograph was used for flood routing, which was derived by historical rainfall runoff process. The time interval is 1 hour. The

https://doi.org/10.5194/hess-2021-470
Preprint. Discussion started: 29 September 2021

Hydrology and Earth System Sciences
Discussions
Open Access
EGU

flood peak, flood volume, and the occurrence time of flood peak are three main basic elements for describing the flood events, and Equation (20) was used as the objective function. The average Nash-Sutcliffe efficiency, relative flood peak error, and peak occurrence time error obtained in the calibration period of the XAJ model are 0.92, 26.1%, and 1.5 hours respectively, indicating a good performance of the XAJ model. The detailed information of the calibrated parameters of the XAJ model is shown in Table 2.

4.1.2 Parameters determination of the proposed flood routing method

As mentioned in Section 2.2, the core of the DUH is the calculation of grid flow velocity. As shown in Equation (15), the parameters that need to be calibrated are K, S, I_c and γ, in which I_c can be determined according to the hourly mean rainfall intensity and flood forecast accuracy of the target basin. For the Qin River Basin, the I_c is set to 20 mm/h, because the mean rainfall intensity of multiple floods is about 20mm/h. Additionally, parameter γ reflects the influence of soil moisture content in unsaturated regions on flow velocity. The smaller of parameter γ is, the smaller the influence of soil moisture content has on the flow velocity. When the value of γ is equal to 1, the flow velocity of grid cell is proportional to the soil moisture content factor w_t. According to the previous research on the flow velocity, the effect of upstream contributions on the flow velocity is adjusted by a coefficient, which is set to 0.5. Inspired by the research, the parameter γ of soil moisture content is assumed to be 0.5 to reflect the influence of soil moisture content on flow velocity in this study

(Bhattacharya et al., 2012; Bunster et al., 2019). In order to determine the grid cell slope *S*, the slope distribution of the study areas is obtained from the DEM data of the target basin as shown in Figure 6(a). Parameter k is the velocity coefficient, which can be determined based on different underlying surface types or different flow states (Ajward & Muzik, 2000). Parameter k changes with different underlying surface types and the detailed k values are given in Table 3. The land type of the Qin River Basin is shown in Figure 6(b). Then the k values of each grid cell can be determined combining Figure 6(b) and Table 3.

The grid flow velocity can be calculated by Equations (1) and (9) with the above parameter settings. In this basis, the flow travel time can be determined by Equation (2). It is noteworthy that the raster size of the basin was divided by 1km×1km, and the rasterized flow direction of each sub-watershed is shown in Figure 6(c), where L is 1 when the rasterized flow is flowing along the edges of the grid, and L is $\sqrt{2}$ when it is diagonally.

4.2 Derivation of TDUH considering time-varying soil moisture content

After determining the parameters above, the flood routing can be calculated based on the proposed TDUH considering time-varying soil moisture content. Meanwhile, in order to improve the efficiency and effectiveness of the routing method, the rainfall intensity and soil moisture content parameters were discretized in present study (Kong et al., 2019). Then a simplified TDUH considering time-varying soil moisture content and TDUH can be obtained in a certain range of rainfall intensities or soil moisture contents, the division ranges of which are presented in Tables 4 and 5. Furthermore, to evaluate the flood simulation effect of the proposed method, the traditional DUH and TDUH methods were used for comparisons.

The DUH without considering rainfall intensity and soil moisture can be obtained based on Equations (1) to (4). Results of the DUH for each sub-watershed of the Qin River Basin are shown in Figures 7. There is only one DUH for a specific sub-watershed due to the simplification of the underlying surface such as slope and land covers. The differences among the DUHs are mainly reflected in the flood peaks and their occurrence time. It can be also seen from Figure 7 that the peaks of DUHs in Sub-watersheds 4 and 6 are significantly lower than others. The reasons may be that the smaller mean slop values of Sub-watersheds 4 and 6 lead to lower flow velocity, resulting in lower peaks of DUH.

Moreover, the TDUHs corresponding to different rainfall intensities of 9 sub-watersheds are shown in Figure 8. It can be seen from Figure 8 that different rainfall intensities correspond to different TDUHs. The increased rainfall intensity leads to higher peak and earlier peak occurrence time of the TDUH. This is because that larger rainfall intensity causes larger flow velocity according to Equation (9). In the practical use of TDUH, the unit hydrographs need to be selected according to the rainfall intensities.

The TDUH of each sub-watershed can be further divided according to the soil moisture content. The TDUHs considering soil moisture contents of Sub-watershed 1 are shown in Figure 9. Obviously, under the same rainfall intensity conditions, the soil moisture content is of great importance to the shape, peak value and duration of the TDUH. Specifically, when the proportion of soil moisture content w_t increases, the proposed method considering soil moisture content is accompanied with steeper rising limb, higher peak and shorter duration. After the whole basin is saturated, the TDUH considering the time-varying soil moisture content is the same with the TDUH.

4.3 Comparisons of flood routing methods

The runoff generation module of the XAJ model was used to calculate the excess rainfall, and the DUH, TDUH and improved TDUH considering soil moisture content were employed for flood routing calculation, respectively. Dozens of floods for the Qin River Bains were applied for model validation. Simulated results of the three methods are shown in Table 6. Three criterions given in Equations (16), (17) and (19) were used for model performance evaluation. It is demonstrated that the proposed method shows the best performance. The relative flood peak error of the proposed method ranges from -3.9% to 9.5%. The mean peak occurrence time error of the proposed is 1.2h, which is the smallest among the three methods. The average NSE coefficients of floods for validation are above 0.8. Figure 10 shows the flood hydrographs of three routing methods for part of the flood events (Event No. 20130720, 20130817, 20150709, 20160128, 20161021 and 20180916). It generally shows the proposed method performs the best among the three routing methods.

The flood events No.20161021 and 20180916 were conducted in-depth analyses for the reason that the forecast results of the both floods using proposed method are not as good as TDUH. For the flood event No.20161021, the simulation result of the proposed method are basically consistent with that of the DUH method. The rainfall in the previous 30 days before the flood event No.20161021 was calculated, and the result shows that the soil moisture content was close to saturation. As mentioned above, for watershed where the soil moisture content is completely saturated, the proposed method performs the same as the TDUH method. Thus, the simulation results of the proposed method and TDUH are almost consistent and better than that of the DUH method for the flood No.20161021. For the flood event No.20180916, there is a lag in the peak time of the proposed method, and the rainfall in the previous time of this flood is relatively small. The possible reason for the inaccurate flood simulation is that the runoff generation is not dominated by the saturation-excess, and it is therefore not appropriate to calculate runoff with the XAJ model.

4.4 Influence of time-varying soil moisture content on floods forecasts

In order to explore the mechanism of time-varying soil moisture content on the flood forecasts, three typical flood forecasting results of the proposed method were chosen for comparison. Specifically, compared with the forecasting results using TDUH, the result of the flood event No.20130817 using the proposed method is relatively similar, the results of the flood events No.20150709 and 20160128 have a better performance, and the result of the flood event No.20180916 is poor. Their corresponding temporal evolution processes of soil moisture content in unsaturated regions were obtained. The box-and-whisker plots of soil moisture contents of all sub-watersheds for flood events No.20130817, 20150709, 20160128 and 20180916 are shown in Figure 11. It can be seen from Figure 11 that the soil moisture content of each sub-watershed is initially low, then the soil moisture content of the sub-watershed gradually increases. Meanwhile, it is obviously that the w_t is hard to reach the maximum. For all the 4 floods, only the flood event No.20130817 does the saturation of 9 sub-watersheds eventually reach. The mean values of w_t for the flood events No.20150709, 20160128 and 20180916 range from 0.5 to 0.8, and the soil moisture content does not reach the maximum during the storm events. As shown from the observed flood in Figure 10, the peak discharge of the flood event No.20130817 is larger than those of other floods, reaching 3500 m^3/s, which means that the watershed is more probably reach the saturation during the flood period.

As discussed in Section 4.3, the result of the flood event No.20130817 using the proposed routing method shows the same behavior as that of TDUH. This is because the simulation performance of the proposed method considering time-varying soil moisture content is the same as the TDUH when the soil moisture contents are closer to 1. Additionally, the forecasting results of the flood events No.20150709, 20160128 with the proposed routing method are obviously better than those of DUH and TDUH. The reason can be summarized as follows. The mean values of w_t range from 0.5 to 0.6 for the two floods and the initially w_t values are low as shown in Figure 11. Thus, the

https://doi.org/10.5194/hess-2021-470
Preprint. Discussion started: 29 September 2021

soil moisture content has a significant impact on the shape of hydrographs. For the flood event No.20180916, the sub-watersheds do not reach a global saturation eventually, and the time-varying values of w_t are generally high, which leads to lower flow velocity than that of the TDUH method. The peaks occurrence time of unit hydrographs used for the runoff routing calculation are general later, and therefore leading to a lag time between the maximum rainfall intensity and the peak discharge for the forecasting result of the flood event No.20180916. The flood peak discharge is higher, which may be due to the inaccurate calculation of excess rainfall.

4.5 Comparisons of velocity calculated by the three routing methods

The routing method considering both time-varying rainfall intensity and soil moisture content is more accurate as discussed in Section 4.3. To explore the effect of time-varying soil moisture content on flow velocity, we selected a grid cell in the Sub-watershed 3, in which slope and land type parameters are constants. Then, the flow velocity was calculated under different storm conditions. The storm events No.20130817 and 20150709 were selected and compared, because the storm event No.20130817 is with a high intensity and long duration, and the storm event No. 20150709 is with a short period of heavy rainfall. Thus, soil moisture contents during the two storm events are significantly different. Figure 12 shows time-varying velocity values of a grid cell for storm events No.20130817 and 20150709. For the two storm events, the mean velocity of the DUH method is the largest among the three methods, followed by the TDUH method. The velocity calculated by the proposed method considering soil moisture content is the smallest. The velocity of DUH method is a constant in two storms, and that of the TDUH method varies with the changes of the excess rainfall. Meanwhile, the flow velocity of the proposed method is not only dominated by rainfall intensity, but also related to soil water content.

For the storm event No.20130817, the initial soil moisture content is large, and it reaches the maximum rapidly. The flow velocity of the proposed method is slightly smaller than that of TDUH method at the initial stage of storm events. When the whole basin reaches saturation, the flow velocity of the two methods is equal. Therefore, the differences of hydrographs are small when using TDUH method and the proposed method for flood routing calculation, which leads to similar forecasting results.

For the storm event No.20150709, the initial soil moisture content is small, and the entire basin cannot reach the saturation after the rainstorm. Therefore, the grid velocity in the early stage of a storm is greatly affected by the soil moisture content. In the later stage of the rainstorm, the w_t of the watershed does not reach the maximum, and it is nearly close to 1. Thus, the impact of later soil moisture content on the flow velocity value is small. From the analyses above, it can be concluded that the shape and duration of the unit hydrograph is mainly related to the soil moisture content at the initial stage of a storm, and when the watershed is approximately saturated, the grid flow velocity is majorly dominated by the excess rainfall.

https://doi.org/10.5194/hess-2021-470
Preprint. Discussion started: 29 September 2021

4. Conclusions

An improved distributed unit hydrographs routing method considering time-varying soil moisture content was proposed for flood routing. The proposed method comprehensively considered the changes of time-varying soil moisture content and rainfall intensity. The response of underlying surface to the soil moisture content was considered as an important factor in this study. The Qin River Basin was selected as a case study. The DUH, TDUH and proposed routing methods were used for flood forecasts, and the simulated results were compared and discussed. The main conclusions are summarized as follows.

(1) The proposed runoff routing method considering both time-varying rainfall intensity and soil moisture content was proposed, and the influence of the inhomogeneity of runoff generation on the confluence process was considered. It is suggested that the soil moisture content is a significant factor affecting the accuracy of flood forecasts, especially in the catchment dominated by saturation-excess runoff, and the flow velocity increases gradually with more surface runoff after considering the soil moisture content in unsaturated regions.

(2) The time-varying characteristics of the DUH can be further considered by introducing both the factors such as rainfall intensity and soil moisture content to the flow velocity formula, which can effectively improve the accuracy of flood forecasts. The simulation hydrographs and criterions of ten floods show that the accuracy of the proposed method is the highest, followed by the TDUH method, and then the DUH

https://doi.org/10.5194/hess-2021-470
Preprint. Discussion started: 29 September 2021

method.

(3) The shape and duration of the improved TDUH considering soil moisture are mainly affected by the rainfall intensity. Meanwhile, soil moisture content at initial stage of a storm also plays a significant role in the characteristics of the improved TDUH. When the watershed is approximately saturated, the grid flow velocity is majorly dominated by the excess rainfall.

Data availability

Due to the strict security requirements from the departments, some or all data, models, or code generated or used in the study are proprietary or confidential in nature and may only be provided with restrictions (e.g. anonymized data).

Author contributions

Lu Chen conceived the original idea, and Bin Yi designed the methodology. Ping Jiang collected the data. Bin Yi developed the code and performed the study. Bin Yi, Lu Chen, and Hansong Zhang contributed to the interpretation of the results. Bin Yi wrote the paper, and Lu Chen revised the paper.

Competing interests

The authors declare that they have no conflict of interest.

Acknowledgments

This research has been supported by the key project of Natural Science Foundation of

China (No. U1865202, No. 52039004).

References

Alfieri, L., Burek, P., Feyen, L. and Forzieri, G.: Global warming increases the frequency of river floods in Europe. Hydrology and Earth System Sciences. 19:2247-2260, https://doi.org/10.5194/hess-19-2247-2015, 2015.

Bhunya, P. K., Ghosh, N. C., Mishra, S. K., Ojha, C. S. and Berndtsson, R.: Hybrid Model for Derivation of Synthetic Unit Hydrograph. Journal of Hydrologic Engineering, 10(6):458-467, https://doi.org/10.1061/(ASCE)1084-0699(2005)10:6(458), 2005.

Beskow, S., Mello, C. R., Norton, L. D. and da Silva, A. M.: Performance of a distributed semi-conceptual hydrological model under tropical watershed conditions. Catena, 86(3):160-171, https://doi.org/10.1016/j.catena.2011.03.010, 2011.

Bhattacharya, A. K., McEnroe, B. M., Zhao, H., Kumar, D., and Shinde, C.: Modclark model: improvement and application. Journal of Engineering, 2(7):100-118, https://doi.org/10.9790/3021-0271100118, 2012.

Brenden, J., Stefan H. S., Luc, F., Jeroen, C. J. H. Aerts, Reinhard, M., Wouter Botzen, W. J., Laurens M. B., Georg, P., Rodrigo, R. and Philip, J. W.: Increasing stress on disaster-risk finance due to large floods. Nature Climate Change, 4(4):264-268, https://doi.org/10.1038/nclimate2124, 2014.

Bhuyan, M. K., Kumar, S., Jena, J. and Bhunya, P. K.: Flood Hydrograph with Synthetic Unit Hydrograph Routing. Water Resources Management, 29(15):5765-5782, https://doi.org/10.1007/s11269-015-1145-1, 2015.

Bunster, T., Gironás, J., Niemann, J. D.: On the Influence of Upstream Flow Contributions on the Basin Response Function for Hydrograph Prediction. Water Resources Research, 55 (6), 4915-4935, https://doi.org/10.1029/2018WR024510, 2019.

Clark, C. O.: Storage and the unit hydrograph. Transactions, 69(9):1333-1360, https://doi.org/10.1061/TACEAT.0005800, 1945.

Chow, V. T.: Handbook of applied hydrology. Hydrological Sciences Journal, 10(1), 1964.

Chinh, L., Iseri, H., Hiramatsu, K., Harada, M. and Mori, M.: Simulation of rainfall runoff and pollutant load for Chikugo River basin in Japan using a GIS-based distributed parameter model. Paddy and Water Environment, 11(1-4):97-112, https://doi.org/10.1007/s10333-011-0296-9, 2013.

Dooge, J.: A General Theory of the Unit Hydrograph. Journal of Geophysical Research Atmospheres, 64(2):241-256, https://doi.org/10.1029/JZ064i002p00241, 1959.

Duan, Q. Y., Sorooshian, S., Gupta, V.: Effective and efficient global optimization for conceptual rainfall-runoff models. Water Resources Research. 28(4):1015-1031,

https://doi.org/10.5194/hess-2021-470
Preprint. Discussion started: 29 September 2021

https://doi.org/10.1029/91WR02985, 1992.

Du, J., Xie, H., Hu, Y., Xu, Y. P. and Xu, C. Y.: Development and testing of a new storm runoff routing approach based on time variant spatially distributed travel time method. Journal of Hydrology, 369(1-2):44-54, https://doi.org/10.1016/j.jhydrol.2009.02.033, 2009.

Gupta, V. K., Waymir, E., Wang, C. T.: A representation of an instantaneous unit hydrograph from geomorphology. Water Resources Research, 16(5): 855-862, https://doi.org/10.1029/WR016i005p00855, 1980.

Gibbs, M. S., Dandy, G. C., Maier, H. R.: Evaluation of parameter setting for two GIS based unit hydrograph models. Journal of Hydrology, 393(3-4), 197–205, https://doi.org/10.1016/j.jhydrol.2010.08.014, 2010.

Gironás, J., Niemann, J. D., Roesner, L. A., Rodriguez, F. and Andrieu, H.: A morpho-climatic instantaneous unit hydrograph model for urban catchments based on the kinematic wave approximation. Journal of Hydrology, 377(3-4), https://doi.org/10.1016/j.jhydrol.2009.08.030 317–334, 2009.

Gad, M. A.: Flow Velocity and Travel Time Determination on Grid Basis Using Spatially Varied Hydraulic Radius. Journal of Environmental Informatics, https://doi.org/10.3808/jei.201400259, 23(2):36-46, 2014.

Kumar, R., Chatterjee, C., Singh, R. D., Lohani, A. K. and Kumar, S.: Runoff estimation for an ungauged catchment using geomorphological instantaneous unit hydrograph (GIUH) models. Hydrological Processes, 21(14):1829-1840, https://doi.org/10.1002/hyp.6318, 2007.

Khaleghi, S., Monajemi, P., Nia, M. P.: Introducing a new conceptual instantaneous unit hydrograph model based on a hydraulic approach. Hydrological Sciences Journal, 63:13-14, https://doi.org/10.1080/02626667.2018.1550294, 2018.

Kong, F. Z., Guo, L.: A method of deriving time-variant distributed unit hydrograph. Advances in Water Science, 30(04):477-484, https://doi.org/10.14042/j.cnki.32.1309.2019.04.003. 2019. (in chinese)

Lee, K. T., Chen, N. C., Chung, Y. R.: Derivation of variable IUH corresponding to time-varying rainfall intensity during storms. International Association of Scientific Hydrology Bulletin, 53(2):323-337, https://doi.org/10.1623/hysj.53.2.323, 2008.

Lu, M. J., Li, X.: Time scale dependent sensitivities of the XinAnJiang model parameters. Hydrological Research Letters, 8 (1):51-56, https://doi.org/10.3178/hrl.8.51, 2014.

Laurenson, E. M.: A catchment storage model for runoff routing. Journal of Hydrology, 2(2):141-163, https://doi.org/10.1016/0022-1694(64)90025-3, 1964.

Mockus, V.: Use of storm and watershed characteristics in synthetic hydrograph analysis and application. AGU, Pacific Southwest Region Mtg., Sacramento, Calif, 1957.

Minshall, N. E.: Predicting storm runoff on small experimental watersheds. J. Hydraul. Engng ASCE, 86(HY8), 17-38, https://doi.org/10.1061/JYCEAJ.0000509, 1960.

https://doi.org/10.5194/hess-2021-470
Preprint. Discussion started: 29 September 2021

Maidment, D. R.: Developing a spatially distributed unit hydrograph by using GIS. IAHS publication, 181-181, 1993.

Martinez, V., Garcia, A. I., Ayuga, F.: Distributed routing techniques developed on GIS for generating synthetic unit hydrographs. Transactions of the ASAE, 45(6):1825-1834, https://doi.org/10.13031/2013.11433, 2002.

Maidment, D. R., Olivera, F., Calver, A., Eatherall, A. and Fraczek, W.: Unit hydrograph derived from a spatially distributed velocity field. Hydrological ProcHydrological Processesesses, 10: 831-844, https://doi.org/10.1002/(SICI)1099-1085(199606)10:6<831::AID-HYP374>3.0.CO;2-N, 1996.

Melesse, A. M., Graham, W. D.: Storm runoff prediction based on a spatially distributed travel time method utilizing remote sensing and GIS, Journal of the American Water Resources Association, 40 (4), 863-879, https://doi.org/10.1111/j.1752-1688.2004.tb01051.x, 2004.

Muzik, I.: A GIS-derived distributed unit hydrograph. Hydrological Processes, 10(10):1401-1409, https://doi.org/10.1002/(SICI)1099-1085(199610)10:10<1401::AID-HYP469>3.0.CO;2-3, 1996.

Munich, R. E.: Natural catastrophe losses at their highest for four years, 2017.

Noto, L. V., Loggia, G. L.: Derivation of a distributed unit hydrograph integrating GIS and remote sensing. Journal of Hydrologic Engineering, 12 (6):639-650, https://doi.org/10.1061/(ASCE)1084-0699(2007)12:6(639), 2007.

Nigussie T. A., Yeğen E. B., Melesse A. M.: Performance Evaluation of Synthetic Unit Hydrograph Methods in Mediterranean Climate. A Case Study at Guvenc Micro-watershed, Turkey. In: Melesse A., Abtew W. (eds) Landscape Dynamics, Soils and Hydrological Processes in Varied Climates. Springer Geography. Springer, Cham. https://doi.org/10.1007/978-3-319-18787-7_15, 2016.

Nash, J. E.: The form of the instantaneous unit hydrograph. International Association of Science and Hydrology, 45(3):114-121, 1957.

Paul, P. K., Kumari, N., Panigrahi, N., Mishra, A. and Singh, R.: Implementation of cell-to-cell routing scheme in a large scale conceptual hydrological model Environmental Modelling & Software, 101(C):23-33, https://doi.org/10.1016/j.envsoft.2017.12.003, 2018.

Rodríguez-Iturbe, I., Valdes, J. B.: The geomorphologic structure of hydrologic response. Water Resources Research, 15(6): 1409-1420, https://doi.org/10.1029/WR015i006p01409, 1979.

Rodríguez-Iturbe, I., González-Sanabria, M., Bras R. L.: A geomorphoclimatic theory of the instantaneous unit hydrograph. Water Resources Research, 18(4):877-886, https://doi.org/10.1029/WR018i004p00877, 1982.

Robinson, J. S., Sivapalan, M., Snell, J. D.: On the relative roles of hillslope processes, channel routing, and network geomorphology in the hydrologic response of natural catchments. Water Resources Research, 31(12), https://doi.org/10.1029/95WR01948, 1995.

Rigon, R., Bancheri, M., Formetta, G. and Lavenne, A.: The geomorphological unit hydrograph from a historical-critical perspective[J]. Earth Surface Processes & Landforms, 41(1):27-37, https://doi.org/10.1002/esp.3855, 2016.

Sherman, L. K.: Streamflow from rainfall by the unit-graph method. Engineering News Record, 108:501-505, 1932.

Snyder, F. F.: Synthetic unit-graphs. Transactions American Geophysical Union, 19, 447-454, https://doi.org/10.1029/TR019i001p00447, 1938.

Saghafian, B., Julien, P. Y.: Time to equilibrium for spatially variable watersheds. Journal of Hydrology, 172 (1–4):231-245, https://doi.org/10.1016/0022-1694(95)02692-I, 1995.

SCS. Design of hydrograph. Washington, DC: US Department of Agriculture, Soil Conservation Service. 2002.

Singh, P. K., Bhunya, P. K., Mishra, S. K. and Chaube, U. C.: An extended hybrid model for synthetic unit hydrograph derivation. Journal of Hydrology, 336(3-4):347-360, https://doi.org/10.1016/j.jhydrol.2007.01.006, 2007.

Singh, P. K., Mishra, S. K. and Jain, M. K.: A review of the synthetic unit hydrograph: from the empirical UH to advanced geomorphological methods. International Association of Scientific Hydrology Bulletin, 59(2):239-261, https://doi.org/10.1080/02626667.2013.870664, 2014.

Sarangi, A., Madramootoo, C. A., Enright, P. and Prasher, S. O.: Evaluation of three unit hydrograph models to predict the surface runoff from a Canadian watershed. Water Resources Management, 21(7):1127-1143, https://doi.org/10.1007/s11269-006-9072-9, 2007.

Singh, S. K.: Simple Parametric Instantaneous Unit Hydrograph. Journal of Irrigation & Drainage Engineering, 141(5):04014066.1-04014066.10, https://doi.org/10.1061/(ASCE)IR.1943-4774.0000830, 2015.

Vrugt, J. A., Gupta, H. V., Dekker, S. C., Sorooshiand, S., Wagenere, T. and Boutenf, W.: Application of stochastic parameter optimization to the Sacramento Soil Moisture Accounting model. Journal of Hydrology, 325(1-4),288-307, https://doi.org/10.1016/j.jhydrol.2005.10.041, 2006.

Zhao, R. J., Zuang, Y., Fang, L.: The xinanjiang model. IAHS AISH Publ. 129, 351-356, 1980.

Zhao, R. J.: Xinanjiang model applied in China. J. Hydrol. 135(1-4), 371-381, https://doi.org/10.1016/0022-1694(92)90096-E, 1992.

Zhou, Q., Chen, L., Singh, V. P., Zhou, J. Z., Chen, X. H. and Xiong, L. H.: Rainfall-runoff simulation in Karst dominated areas based on a coupled conceptual hydrological model. Journal of Hydrology, 573: 524-533, https://doi.org/10.1016/j.jhydrol.2019.03.099, 2019.

List of Tables

Table 1. Detailed information of sub-watersheds

Sub-watersheds	Drainage area/km^2	Number of grids	Average slope
Sub-watershed 1	175.64	176	13.29
Sub-watershed 2	195.86	197	9.27
Sub-watershed 3	154.97	156	12.50
Sub-watershed 4	153.08	151	9.57
Sub-watershed 5	147.79	147	12.49
Sub-watershed 6	249.36	253	11.74
Sub-watershed 7	213.34	211	10.56
Sub-watershed 8	122.28	129	10.77
Sub-watershed 9	166.51	161	9.74

720 **Table 2.** Calibrated parameters of the XAJ model

Parameters	Physical meaning	Value	Unit
UM	Averaged soil moisture storage capacity of the upper layer	18.87	mm
LM	Averaged soil moisture storage capacity of the lower layer	73.67	mm
DM	Averaged soil moisture storage capacity of the deep layer	39.29	mm
B	Exponential of distribution of tension water capacity	0.27	-
IM	Ratio of impervious to total areas in the catchment	0.01	-
K	Ratio of potential evapotranspiration to pan evaporation	0.85	-
C	Evapotranspiration coefficient of the deeper layer	0.12	-
SM	Free water capacity of the surface layer	46.29	mm
EX	Exponent of the free water capacity curve influencing the development of the saturated area	0.50	-
KI	Outflow coefficient of free water storage to interflow	0.41	-
KG	Outflow coefficient of free water storage to groundwater	0.28	-
CI	Recession constant of the lower interflow storage	0.87	-
CG	Recession constant of the ground water storage	0.99	-
CS	Recession constant in the lag and rout method for routing through the channel system within each sub-watershed	0.46	-
KE	Muskingum time constant for each sub-reach	23.90	-
XE	Muskingum weighting factor for each sub-reach	0.13	-

721 **Table 3.** The specific values of *k* for different vegetational types

https://doi.org/10.5194/hess-2021-470
Preprint. Discussion started: 29 September 2021

Land Type	Vegetational Form	k (m/s)
Crop land	fallow	1.37
	contour tillage	1.40
	straight plough	2.77
Grass and plow land	trample	0.30
	lush	0.46
	sparse	0.64
	pasture	0.40
Forest	dense	0.21
	sparse	0.43
	full of dead leaves	076
Impervious surface	\	6.22

722 **Table 4.** The rainfall intensity I_t of each period corresponds to the discrete rain intensity

723 I_s

Net rainfall intensity I_t (mm/h)	$0 < I_t \leqslant 15$	$15 < I_t \leq 25$	$25 < I_t \leq 35$	$I_t > 35$
Discrete rainfall intensity I_s(mm/h)	10	20	30	40

724 **Table 5.** The soil moisture content w_t of each period corresponds to the discrete soil

725 moisture content w_s

Soil moisture content w_t	$0 < w_t \leq 0.2$	$0.2 < w_t \leq 0.4$	$0.4 < w_t \leq 0.6$	$0.6 < w_t \leq 0.8$	$w_t > 0.8$
Discrete soil moisture content w_s	0.1	0.3	0.5	0.7	0.85

726 **Table 6.** The results of three criterions for all routing methods

Event number	***Obj*₁ (%) / *Obj*₂ (h) / *Obj*₃ (-)** DUH	TDUH	Proposed
20130720	13.3/5/0.47	12.5/3/0.52	**-3.9/1/0.73**
20130817	4.7/7/0.69	0.5/4/0.81	**4.9/2/0.82**
20130922	15.9/-3/0.57	-11.1/-3/0.54	**2.4/2/0.85**
20150709	27.1/-3/0.56	-18.8/0/0.54	**9.5/-1/0.83**
20160128	1.7/1/0.32	-6.6/-1/0.48	**1.5/0/0.92**
20160827	8.8/2/0.75	4.9/1/0.81	**3.3/0/0.91**

https://doi.org/10.5194/hess-2021-470
Preprint. Discussion started: 29 September 2021

Hydrology and Earth System Sciences
Open Access
EGU
Discussions

20161021	15.7/3/0.56	**4.6/-1/0.78**	8.8/-2/0.72
20180606	4.8/2/0.64	-2.4/1/0.72	**2.6/0/0.84**
20180830	4.2/-2/0.71	**-0.3/-1/0.82**	2.4/1/0.79
20180916	6.5/8/0.52	**-4.8/3/0.69**	4.4/-3/0.54
Average	|9.5|/|3.3|/0.58	|7.4|/|2.1|/0.67	**|4.4|/|1.2|/0.80**

List of Figures

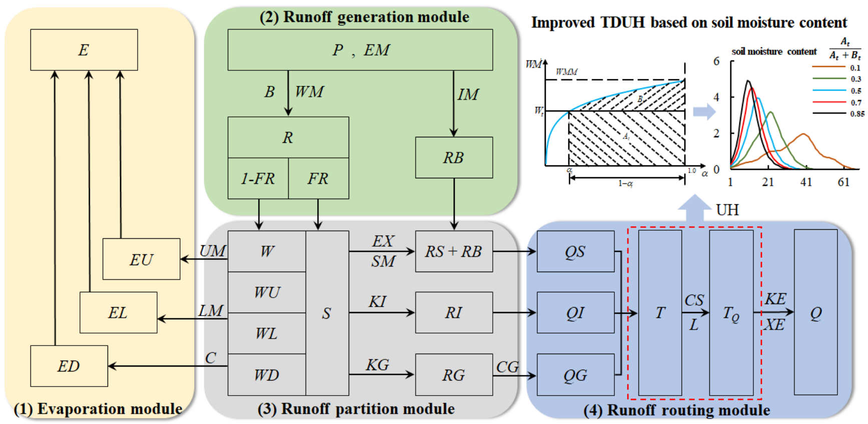

Figure 1. Schematic diagram of the XAJ model

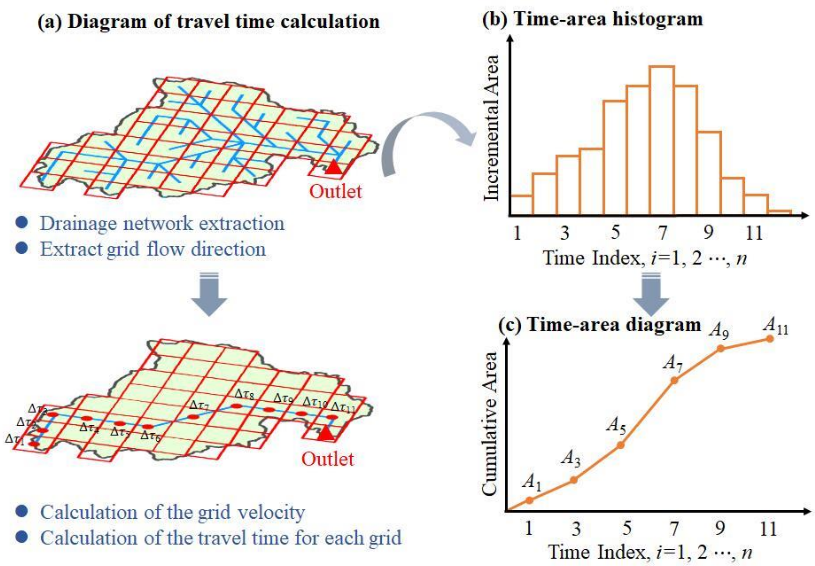

Figure 2. Schematic diagram of the DUH

732 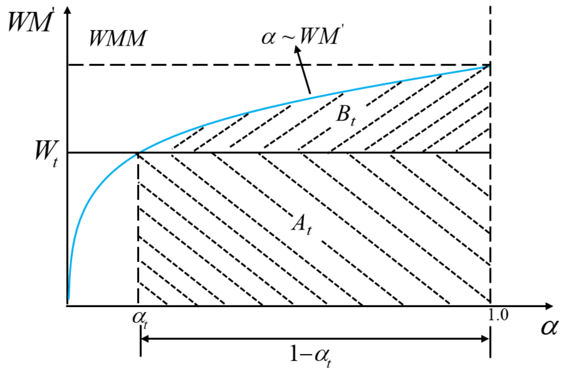

733 **Figure 3.** Watershed storage capacity curve

734 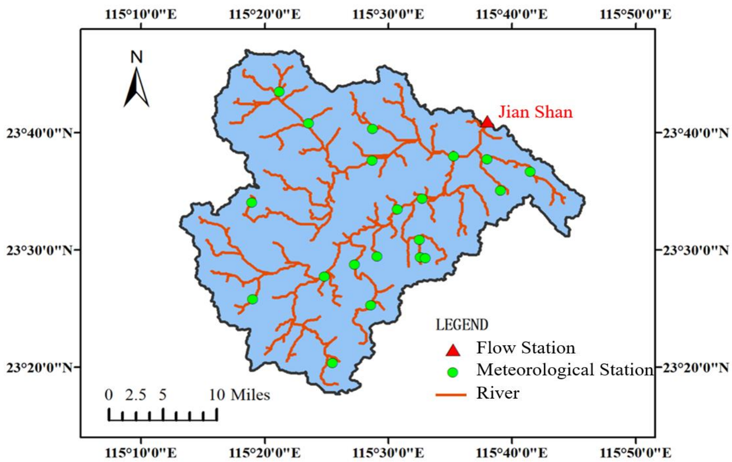

735 **Figure 4.** Distribution diagram of meteorological and flow stations in Qin river basin

736 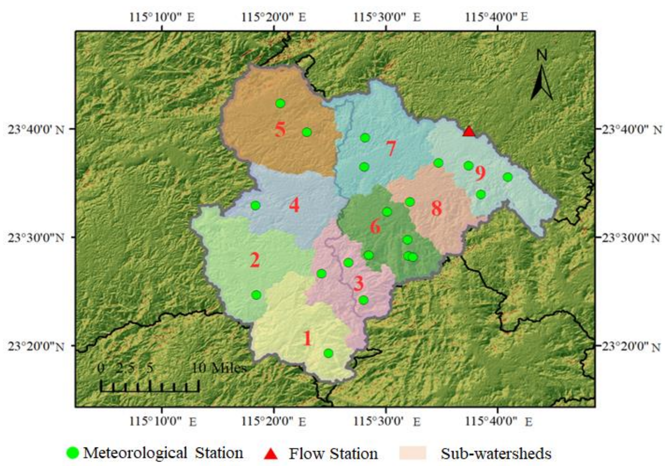

https://doi.org/10.5194/hess-2021-470
Preprint. Discussion started: 29 September 2021

Figure 5. The sub-watershed of the Qin River Basin. (*Note*. The satellite imagines for the study area are available at http://www.gscloud.cn)

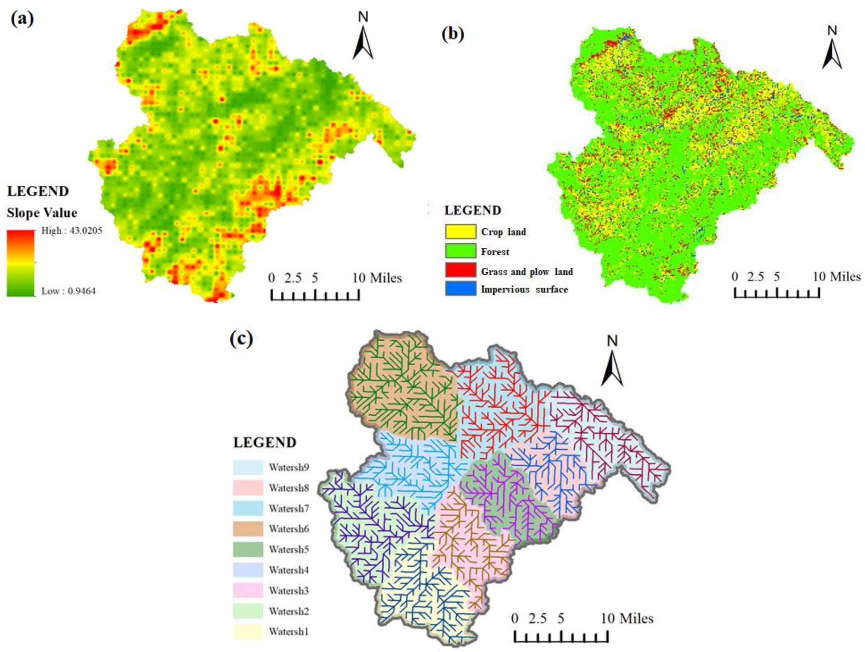

Figure 6. Slope, Land types and rasterized flow direction of the Qin River Basin. (a) Slope distribution. (b) Land types. (c) Rasterized flow direction.

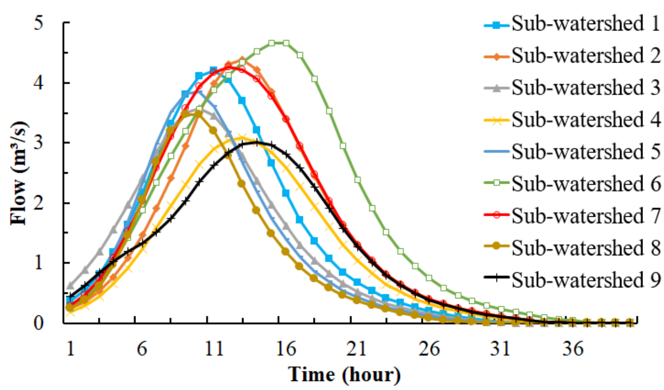

Figure 7. The DUH for the Qin River Basin

https://doi.org/10.5194/hess-2021-470
Preprint. Discussion started: 29 September 2021

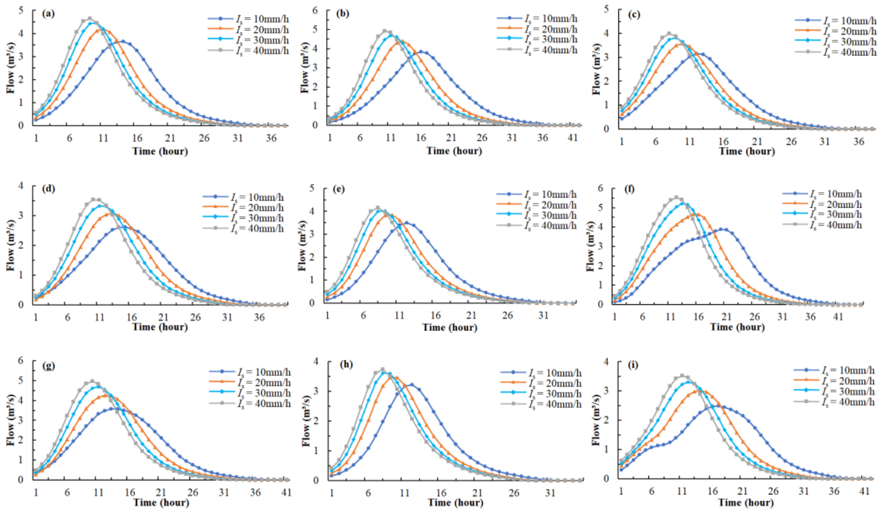

Figure 8. The TDUH for the Qin River Basin. (a) Sub-watershed 1. (b) Sub-watershed 2. (c) Sub-watershed 3. (d) Sub-watershed 4. (e) Sub-watershed 5. (f) Sub-watershed 6. (g) Sub-watershed 7. (h) Sub-watershed 8. (i) Sub-watershed 9.

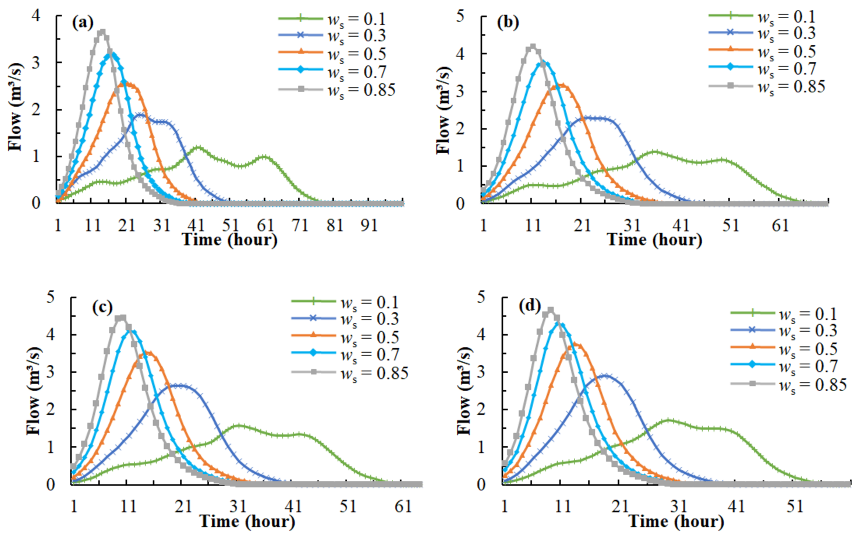

Figure 9. The TDUH considering soil moisture content for sub-watershed 1 of Qin River Basin. (a) $I_s = 10\text{mm/h}$. (b) $I_s = 20\text{mm/h}$. (c) $I_s = 30\text{mm/h}$. (d) $I_s = 40\text{mm/h}$.

https://doi.org/10.5194/hess-2021-470
Preprint. Discussion started: 29 September 2021

Hydrology and Earth System Sciences
Discussions
Open Access

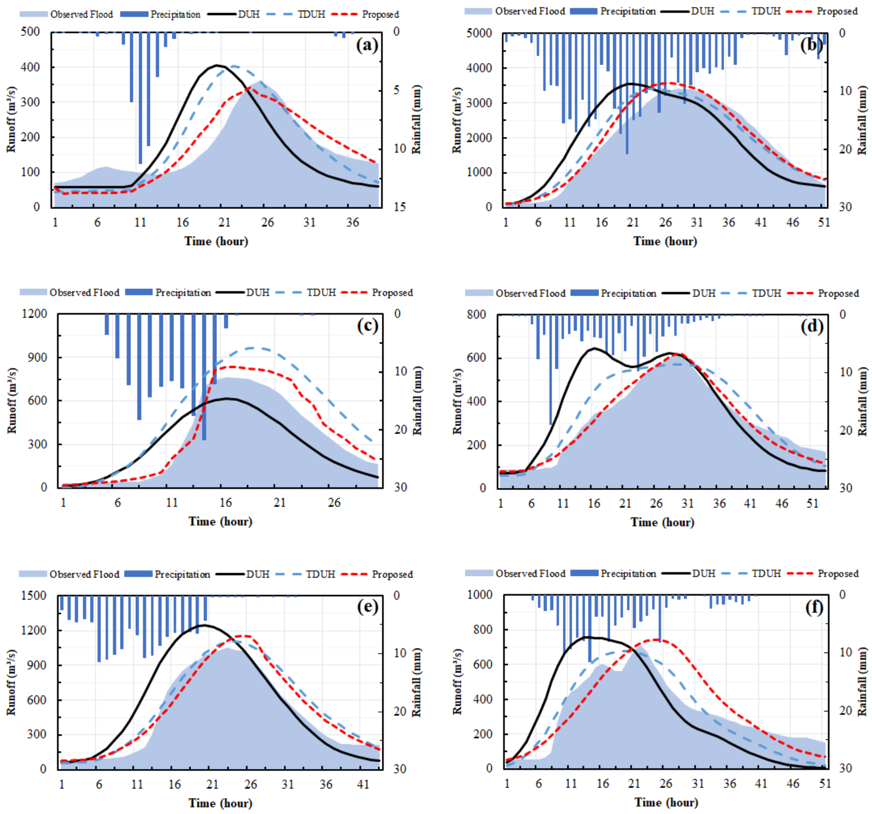

Figure 10. Comparisons of flood hydrograph obtained by three methods. (a) Flood event No.20130720. (b) Flood event No.20130817. (c) Flood event No.20150709. (d) Flood event No.20160128. (e) Flood event No.20161021. (f) Flood event No.20180916.

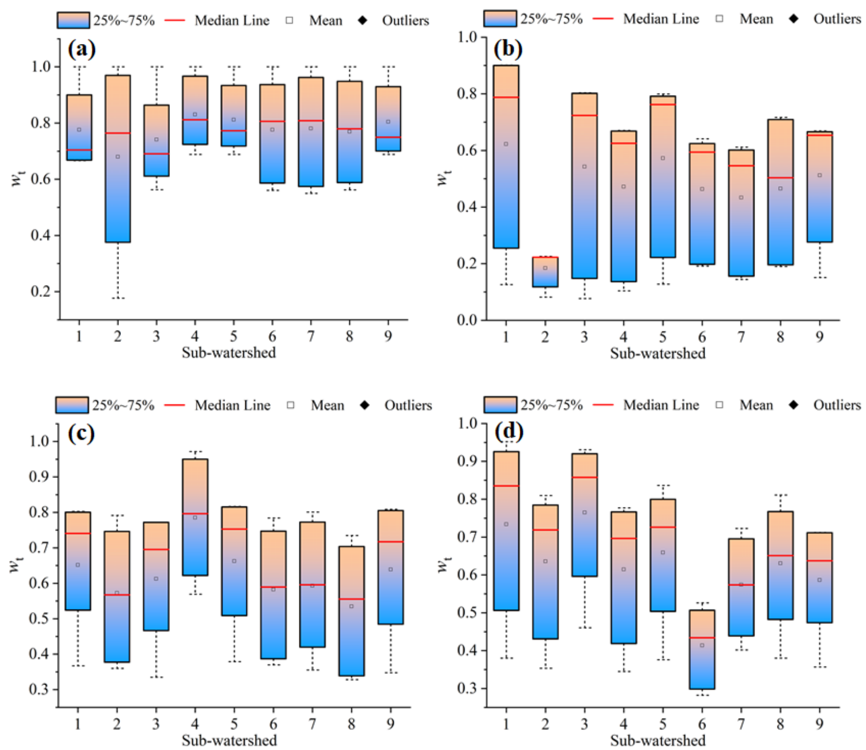

Figure 11. Distributions of time-varying w_t at different times in each sub-watershed during the simulation period of the runoff using proposed TDUH method. (a) Flood event No.20130817. (b) Flood event No.20150709. (c) Flood event No.20160128. (d) Flood event No.20180916. w_t represents the ratio of current soil moisture content to the corresponding maximum soil moisture content in unsaturated region.

https://doi.org/10.5194/hess-2021-470
Preprint. Discussion started: 29 September 2021

Hydrology and Earth System Sciences
Open Access
EGU
Discussions

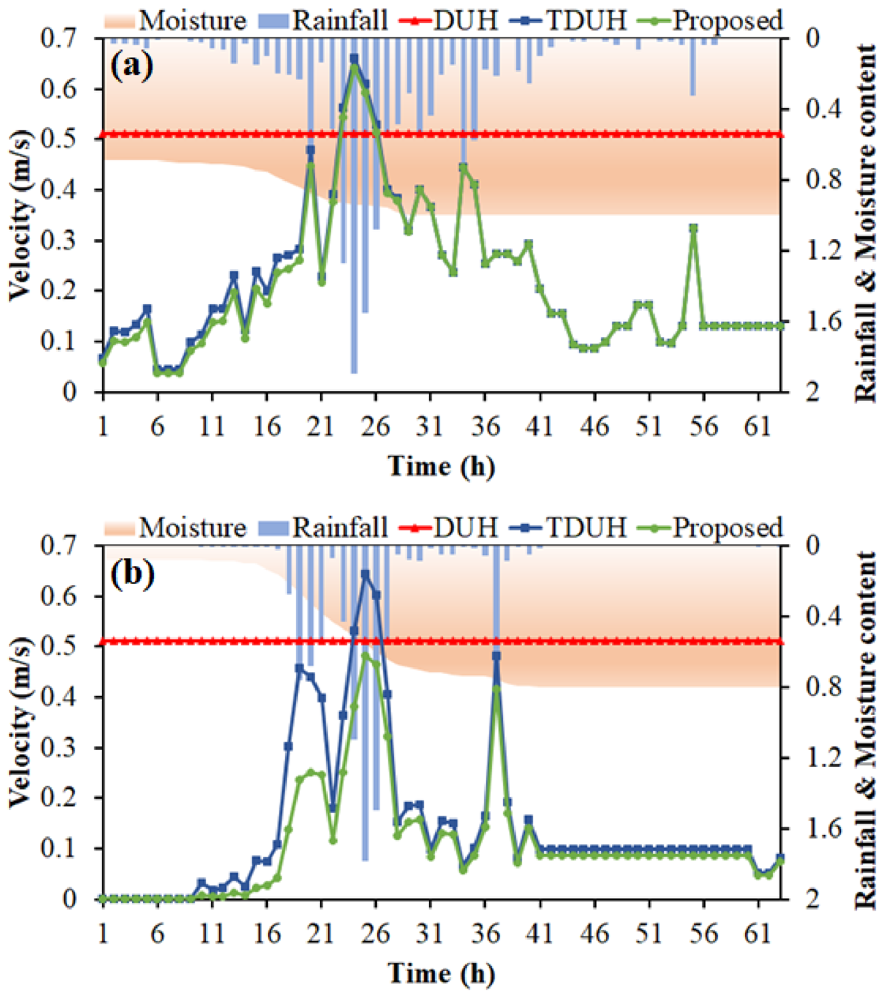

768

769 **Figure 12.** Time-varying velocity values of a grid cell in different storm events. (a)
770 Time-varying velocity in storm event No.20130817. (b) Time-varying velocity in storm
771 event No.20150709. The rainfall content is $\frac{I_s}{I_c}$, and the soil moisture content is w_t.